Published in Journal of Non-Crystalline Solids 266-269, 125-130, 2000
which should be used for any reference to this work

Microstructure and surface roughness of microcrystalline silicon prepared by very high frequency-glow discharge using hydrogen dilution

E. Vallat-Sauvain *, U. Kroll, J. Meier, N. Wyrsch, A. Shah

Institut de Microtechnique, Université de Neuchâtel, rue Breguet 2, 2000 Neuchâtel, Switzerland

Abstract

The microstructure of a series of silicon films deposited by very high frequency glow discharge (VHF-GD) with silane concentration in hydrogen varying from 100% down to 1.25% has been observed with transmission electron microscopy (TEM). The surface topography of the layers has been analysed by atomic force microscopy (AFM). At silane concentration below 8.6%, a phase transition between amorphous hydrogenated silicon (a-Si:H) and microcrystalline silicon (μc-Si:H) is observed by TEM. After this transition, the further decrease of silane concentration leads to complex changes of the crystalline microstructure of the layers. AFM observations of the surface reveal that the film rms roughness increases with the decrease of the silane concentration. The surface morphology is not related simply to the microstructure of crystalline grains as observed by TEM.

1. Introduction

As shown by Veprek in 1968, microcrystalline hydrogenated silicon (μc-Si:H) can be directly deposited at low temperature [1]. Since then, μc-Si:H has found more applications as doped layers in solar cells and in thin film transistors. Recently, the application in solar cells of intrinsic μc-Si:H deposited by very high frequency glow discharge (VHF-GD) with silane diluted in hydrogen has been successfully proven [2]. Despite the success of this material as an active absorber in photovoltaic devices [3], relatively little is known about its microstructure [4,5] and the link between the material microstructure and the device performance is still lacking. The aim of this paper is to present the effect of the dilution of silane on the microstructure and on the surface morphology of μc-Si:H layers deposited on glass substrates. Our TEM observations show many different types of microstructures in a series of samples deposited at silane dilution levels within the range used in practice for the deposition of the *i*-layers in solar cells. Surface morphology of the layers is also an important parameter for device performance. Indeed, a rough layer allows for an increased light trapping in the active *i*-layer of the cell, thereby to an increased short-circuit current [6].

* Corresponding author. Tel.: +41-32 718 33 59; fax: +41-32 718 32 01.
E-mail address: evelyne.vallat@imt.unine.ch (E. Vallat-Sauvain).

2. Experimental

Films were deposited in a capacitively-coupled parallel plate reactor using a plasma excitation frequency of 70 MHz. The silane concentration in the feed gas was varied from 100% down to 1.25% by adapting the ratio of the silane and hydrogen flows, while keeping the total feed gas constant at 50 scm. The depositions of 1.5–2 μm-thick films on Corning 7059 glass substrates were performed at a pressure of 0.4 mbar, a HF-power input of 7 W and a substrate temperature of 225°C. These films have been characterised by Infrared spectroscopy, elastic recoil detection analysis (ERDA) and X-ray diffraction [7,8].

The conventional TEM sample preparation by the ion-milling method is known to amorphize silicon nanocrystals and to preferentially etch around cracks [9]. To avoid these artefacts, we scraped the films from the glass substrate and directly placed the fragments on a carbon-coated TEM grid. The drawback of this technique is that fracture along the growth direction cannot be controlled. As a consequence, inhomogeneities on the sample's surface (like the protrusions in Fig. 5) may be harder to observe than the above mentioned conventional preparation technique. The grids were examined in a electron microscope (Philips CM200) operated at an accelerating voltage of 200 kV. AFM studies were performed with a commercial microscope in the non-contact mode.

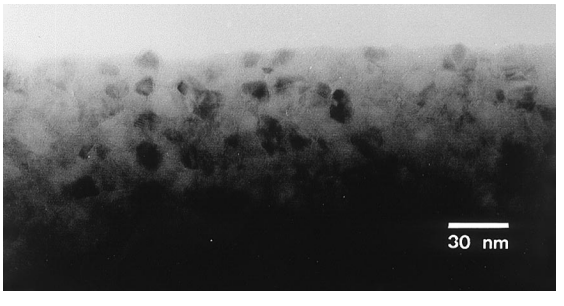

Fig. 1. Plane view bright field micrograph of the sample prepared at a silane concentration of 7.5%. It exhibits small crystallites (dark dots of 10 nm diameter, standard deviation ±4 nm) embedded in an amorphous matrix. The crystalline surface density is about 10%.

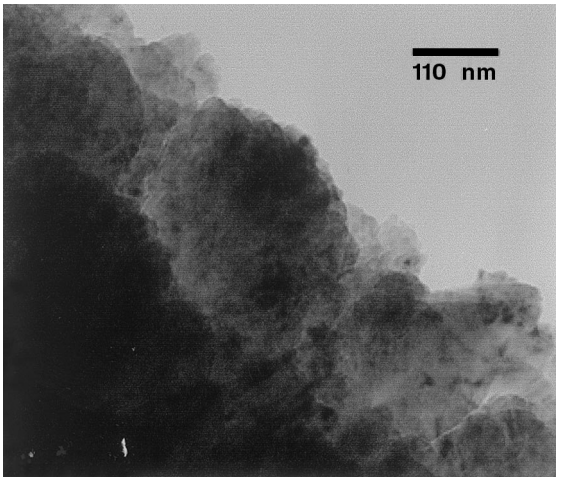

Fig. 2. Cross-section bright field micrograph of the sample prepared at a silane concentration of 2.5% exhibiting large (200 nm diameter) bunches of grains (average diameter of 28 nm, standard deviation ±27 nm), resulting in a rough sample-air interface. One leaf-like shaped grain pointing out of the sample can be identified.

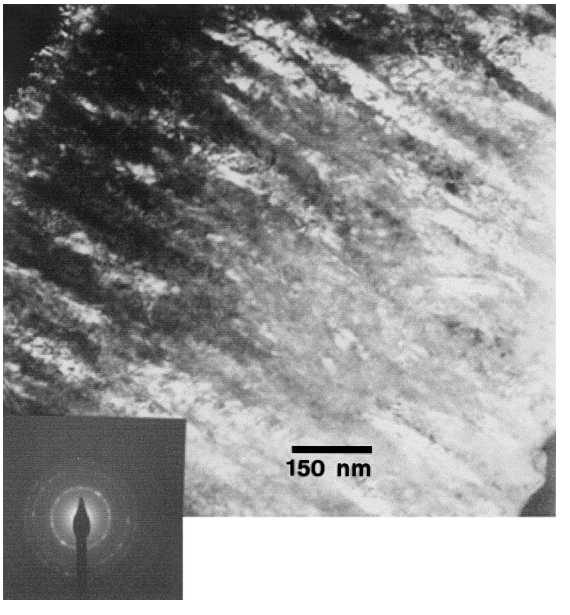

Fig. 3. Cross-section dark field micrograph of the sample prepared at a silane concentration of 1.25%. Columnar grains of 750 nm length can be observed. The microstructure over the first 40 nm close to the substrate-layer interface (upper left corner) is different: it exhibits a much smaller grain size distribution. The selected area diffraction pattern in inset, composed of dotty rings, is characteristic of the microcrystalline nature of the sample.

3. Results

3.1. TEM observations

Plane view bright field electron micrograph of the 7.5% dilution sample is given in Fig. 1. This sample contains crystallites (nanocrystallites with an average diameter of 10 nm, embedded in an amorphous phase. Cross-sectional observations (not shown) reveal that these nanocrystals are elongated with an average length of 30 nm). Image analysis of this micrograph gives a surface crystalline fraction of about 10%. As the elongated crystallites have roughly the same length as the estimated thickness of the electron transparent edge, the volume crystalline fraction is approximately to the surface crystalline fraction. This sample has an absorption curve that is between the absorption curves for μc-Si:H and for a-Si:H [7,8]. On the other hand, only a very faint X-ray signal indicative of crystallinity was observed [7,8].

Fig. 2 shows the microstructure of the 2.5% dilution sample. Crystallites have an average diameter of 28 nm. The residual amorphous fraction in this sample (as well as in the larger dilution samples) could no longer be estimated from our medium resolution TEM pictures. We observe another feature in this sample: leaf-like grains pointing out of the sample. The latter are rather large monocrystals (150 nm diameter, 350 nm long) with a central symmetry axis consisting of a stacking fault. A similar microstructure had already been observed in thermally recrystallized amorphous silicon samples for TFT applications [10]. Dendritic growth with mostly a (2 2 0) crystallographic texture has been suggested in Ref. [10] for these samples. Note that a predominant (2 2 0) crystallographic texture is also observed in this sample [7,8].

The microstructure of the 1.25% dilution sample is illustrated in Fig. 3. It has long (750 nm length) columnar grains. The average diameter of these long grains is 24 nm. Cracks extending a long way down the grains are present. Our medium resolution micrographs do not show if these cracks are voids or are filled with a thin amorphous tissue. A discontinuity of the microstructure is observed in the first 40 nm close to the glass–silicon

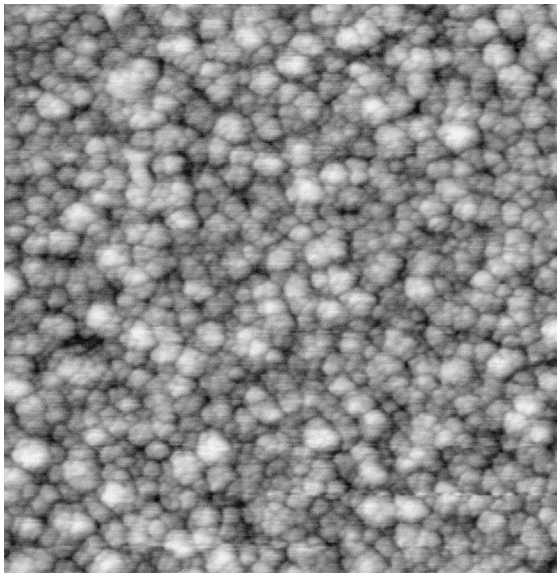

Fig. 4. AFM non-contact measurement of the surface topography of the sample prepared at a silane concentration of 8.6%. The scanned area is 3 μm × 3 μm. It shows grains of 90 nm average diameter and clusters of (in average) three grains. The rms roughness of this sample is 2 nm.

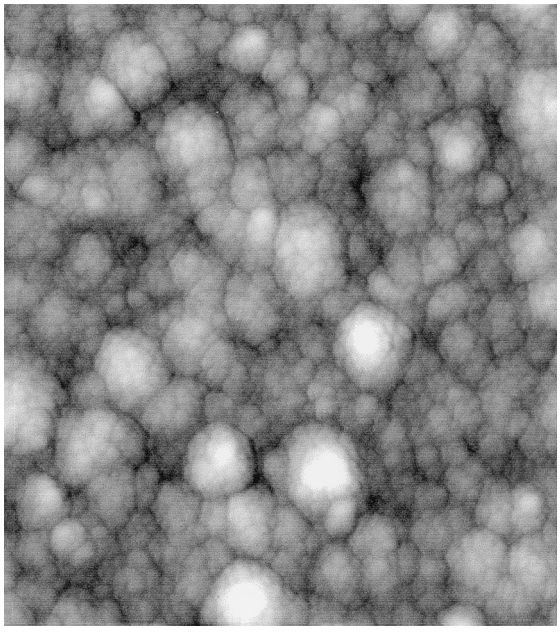

Fig. 5. AFM topography of the sample prepared at a silane concentration of 7.5%. The scanned area is 3 μm × 3 μm. It shows coley-flower like protrusions (bright) composed of smaller grains.

interface: this part of the layer consists of small isotropic grains, indicative of a distinctive nucleation process in this sample.

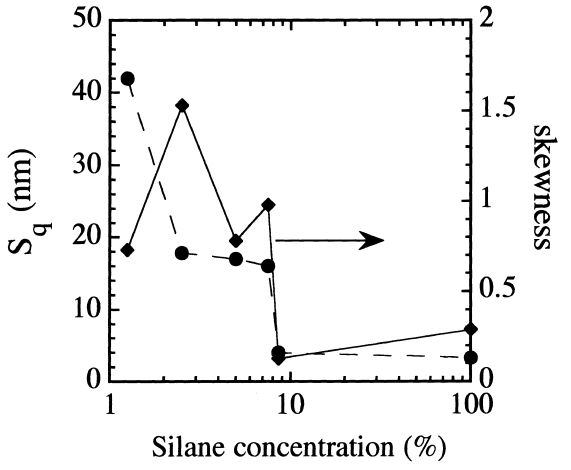

Fig. 6. Rms rougness of the samples surface and skewness of the sample height distribution as a function of the concentration of silane in the plasma gas phase.

3.2. AFM observations

Fig. 4 shows the surface morphology of the a-Si:H sample prepared with 8.6% silane; it looks very similar to that of device quality a-Si:H layers prepared with pure silane. It consists of small grains of 70 nm average diameter, with a rms roughness of 2 nm. The surface morphology of the sample prepared with 7.5% silane is shown in Fig. 5. We observe the occurrence of protrusions of clusters of small grains (in the whole dilution series, the clusters have in average a diameter three times larger than that of the grains). These clusters are emerging from the surface, as expressed by the increase of the skewness of the sample's height distribution (Fig. 6). This parameter expresses the asymmetry of a statistical distribution around its mean. It becomes increasingly positive (asymmetric tail on the positive side of the distribution) for samples consisting of features pointing out of a flat substrate (mesa-like morphology). The general trend in the surface morphology is the following: at the amorphous–microcrystalline transition, the rms roughness increases abruptly. The microcrys-

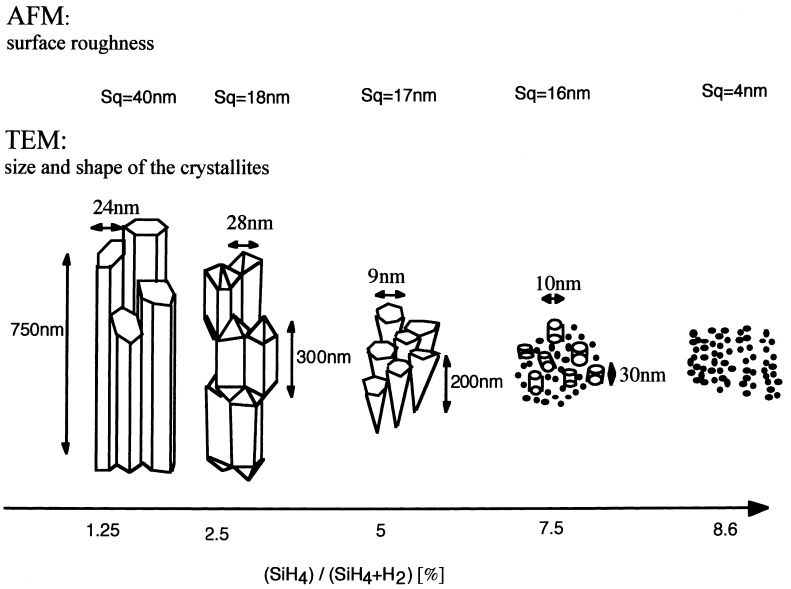

Fig. 7. Schematical representation of the evolution of the microstructure of the layers as a function of the silane concentration in the plasma gas phase. The small black dots represent the amorphous phase. The TEM micrographs of the sample prepared with 7.5% silane are not shown here.

talline samples have larger clusters emerging from the surface (mesa-like) with a coley-flower morphology. By decreasing further the silane concentration the mesa-like morphology disappears and the rms roughness increases.

4. Discussion

The evolution of the microstructure with the silane dilution as observed by TEM is given schematically in Fig. 7. It was generally assumed that μc-silicon is constituted either of microcrystallites of a more or less spherical shape embedded in an amorphous tissue, or of columnar grains extending all the way through the layer, as observed in Ref. [4]. Our study reveals a much larger variety of microstructures. In particular, based on the occurrence of dendritic growth under VHF deposition conditions, similar to that observed in thermally recrystallised a-Si:H samples we suggest that VHF-GD deposition conditions are smooth. However, the detailed growth mechanisms responsible of this variety of crystalline microstructure are not known. Furthermore, the growth mechanisms are dependent (for a given silane concentration) on the type of underlayer (transparent conductive oxide such as ZnO or SnO_2, p-doped layer) on which deposition takes place [11], as well as on the other deposition parameters (frequency, power, temperature [12]). Thus care has to be taken when transferring our observations to other substrates or deposition conditions.

The results of the non-contact AFM topography measurements are summarised in Fig. 6. The amorphous–microcrystalline transition can be identified by an abrupt change in the rms roughness. Surface grains can be seen in AFM pictures (Figs. 4 and 5). The average diameter of the smallest grains in samples exhibiting a coley-flower like surface morphology is, in general, not correlated with the crystallite size observed by TEM (Fig. 8). This result is already known from the comparison of scanning electron microscopy (SEM) images of the surface topology with TEM micrographs [13]. However, in some cases, as dendritic growth occurs (2.5% dilution sample), surface morphology reflects the microstructure of

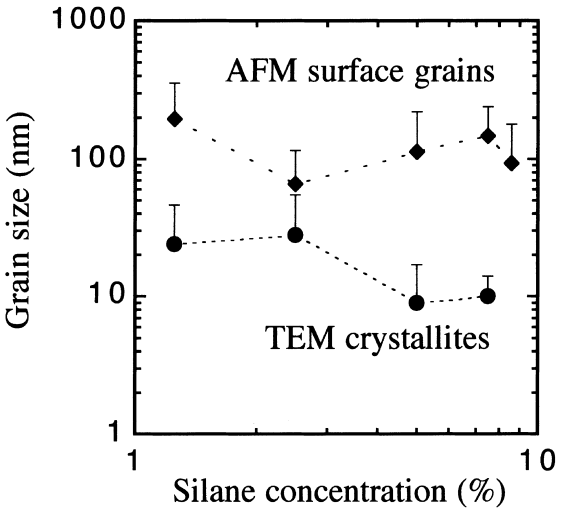

Fig. 8. Grain sizes measured on TEM micrograph and AFM topography measurements. Because of the logarithmic representation, we have plotted only the positive standard deviation by an error bar. The AFM surface grain size is the diameter of the smallest grains (see e.g. Fig. 5).

the sample. In samples close to the amorphous–microcrystalline transition (i.e., of smallest crystalline fraction), the crystallites average diameter as observed by TEM is one order of magnitude smaller than that of the surface grains. Thus, we presume that the surface grains are constituted of a mixture of the two (amorphous and crystalline) phases. For the large dilution samples, where the crystalline fraction is the largest, the average diameter of crystallites as measured by TEM is again smaller than that of the surface grains. Thus, we assume that the surface grains consist of several crystallites.

5. Conclusions

We have studied the microstructure and surface topography of a series of samples deposited at various concentration of silane in hydrogen using the VHF-GD deposition process. TEM observations of the microstructure reveal that for decreasing silane concentration a variety of different microstructures develops. The sample surface topography shows an abrupt increase in the rms

roughness at the amorphous–microcrystalline transition and protrusions out of the surface. It is not straightforward to correlate the sample's surface topography with the layer's microstructure: surface grains are neither single phased in samples close to the transition nor single crystallites in more crystalline samples. However in some cases, when dendritic growth occurs, surface morphology reflects the microstructure of the sample. Our observations of the diversity of microstructures in layers calls now for a study of the *i*-layer microstructure and surface topography in solar cells and their possible effects on the device performances.

Acknowledgements

We thank Professor M. Morris, Professor F. Stöckli and Dr M. Dadras who granted us access to their TEM facilities and S. Dubail for his technical help. We acknowledge financial support from the Swiss Federal Office for Energy BEW/OFEN under grants 2757 and 19431 as well as the Swiss National Science Fund under grant FN52337.

References

[1] S. Veprek, V. Marecek, Solid State Electron. 11 (1968) 683.
[2] J. Meier, R. Flückiger, H. Keppner, A. Shah, Appl. Phys. Lett. 65 (1994) 860.
[3] J. Meier, H. Keppner, S. Dubail, Y. Ziegler, L. Feitknecht, P.Torres, Ch. Hof, U. Kroll, D. Fischer, J. Cuperus, J.A. Anna Selvan, A. Shah, in: Proc. 2nd World Conference and Exhibition on Photovoltaic Solar Energy Conference, vol. 1, Vienna, Austria, 1998, p. 375.
[4] M. Luysberg, P. Hapke, R. Carius, F. Finger, Philos. Mag. A 75 (1997) 31.
[5] L. Houben, M. Luysberg, P. Hapke, R. Carius, F. Finger, H. Wagner, Philos. Mag. A 77 (1998) 1447.
[6] A. Poruba, Z. Remes, J. Springer, M. Vanecek, A. Fejfar, J. Kocka, J. Meier, P. Torres, A. Shah, in: Proc. 2nd World Conference and Exhibition on Photovoltaic Solar Energy Conference, vol. 1, Vienna, Austria, 1998, p. 781.
[7] U. Kroll, J. Meier, P. Torres, J. Pohl, A. Shah, J. Non-Cryst. Solids 69 (1998) 227.
[8] U. Kroll, J. Meier, P. Torres, J. Pohl, A. Shah, J. Appl. Phys. 80 (1996) 4971.
[9] I. Berbezier, Porous Silicon Science and Technology, Les Editions de Physique, Les Ulis, 1994.
[10] M.K. Hatalis, D.W. Greve, J. Appl. Phys. 63 (1988) 2260.
[11] J. Koh, Y. Lee, H. Fujwara, C.R. Wronski, R.W. Collings, Appl. Phys. Lett. 73 (1998) 1526.
[12] A. Matsuda, K. Kumagai, K. Tanaka, Jpn. J. Appl. Phys. 22 (1982) L34.
[13] R. Messier, J. Vac. Sci. Technol. A4 4 (1986) 490.